35th Annual International Conference of the IEEE EMBS
Osaka, Japan, 3 - 7 July, 2013

Simulating the Role of Anisotropy in Human Atrial Cardioversion*

Sanjay R. Kharche, Irina V. Biktasheva, Henggui Zhang, and Vadim N. Biktashev

Abstract— **This computational study quantifies the effectiveness of feedback controlled low energy cardioversion in the anisotropic human atria.**

An established biophysical human cell model was adopted to reproduce Control and chronic atrial fibrillation (CAF) action potentials. The cell model was combined with a detailed human atrial geometry to construct a 3D realistic human atrial model. Scroll waves were simulated under Control and CAF conditions and the cardioversion parameters of stimulation strength and pacing duration were evaluated for scroll wave termination. Scroll waves were initiated at two locations in the atria to elicit the effects of scroll wave location. The role of anisotropy was highlighted by comparison to results from the isotropic case.

Under Control conditions, scroll wave self-termination was rapid in the anisotropic case. Under CAF conditions, anisotropy caused the initiated scroll wave to degenerate into multiple scrolls with each evolving erratically or pinning to anatomical defects. The cardioversion successfully terminated scroll waves within 10 s, but the stimulus strength had a strong correlation to the location of the scroll wave. The low energy stimulation strength was always lower than the threshold stimulus.

Anisotropy plays an important role in atrial electrical properties. Anisotropy aggravates CAF and leads to high frequency atrial pacing. The efficacy of cardioversion is significantly affected by anisotropy.

I. Introduction

Scroll waves are re-entrant electrical circuits in the cardiac wall with a transmural filament at their centre and mechanisms of their genesis have been discussed extensively [1]. Supraventricular tachycardia, like chronic atrial fibrillation (CAF), can be effectively treated using a low energy resonant pacing cardioversion method as suggested by Biktashev and Holden [2]. The underlying theory that describes the interaction of scroll waves with small amplitude stimuli involved in the cardioversion has been developed [3, 4], and also confirmed in the isotropic (i.e. without fibre orientation anisotropy) 3D atrium [5]. However, anisotropy is known to play a significant role in the human atria [6]. The aim of this study was to evaluate the stimulation strength and pacing duration required for successful low voltage cardioversion in the anisotropic atria in comparison to a similar study in the isotropic case [5].

All computer simulations and post processing, apart from visualization were done using the High Performance Computing cardiac simulation environment, Beatbox [7]. Visualization was carried out using Gnuplot and ParaView.

II. Methods

The Courtemanche et al. [8] (CRN) cell model for human atrial action potential (AP) was used in this study. CAF was simulated by reducing the L-type calcium current conductance by 50%, and increasing the time independent outward rectifier potassium current conductance by 100% [9]. This definition of CAF is the same as in the previous simulation results of the isotropic case [5]. Fig. 1A shows AP profiles under Control and CAF electrophysiological conditions. The anisotropic 3D anatomical model of human atria with the fiber orientation anisotropy in the atrial conduction pathways [10] (Fig. 1B) was used for the 3D realistic model. Numerical solutions of scroll wave evolution were obtained using a mono-domain reaction diffusion formulation:

$$C_m dV_m / dt = \nabla \left(\mathbf{D} \nabla V_m \right) - I_{ion} \quad (1)$$

with the no flux boundary conditions

$$\mathbf{n} \cdot \mathbf{D} \nabla V_m = 0 \quad (2)$$

where C_m is the cell capacitance, V_m is the membrane potential, **D(x, y, z)** is the anisotropic diffusion tensor, I_{ion} is the ionic current, and **n** is the unit normal boundary. The human atrial geometry is embedded in a Cartesian grid of 235 x 269 x 298 grid points with space step 0.33 mm and discretisation carried out using a 19 point 3D finite difference stencil. The space discretisation was the same as in the original anatomical model data set [10]. The diffusion was taken to be 0.07 mm^2/ms transverse to fiber direction, and 0.22 mm^2/ms parallel to fiber direction [11] giving a conduction velocity (CV) of 0.33 mm/ms transverse to fibers and 0.57 mm/ms in the direction parallel to fibers. Clinical and experimental measurements indicate higher values of CV [11]; however, there are also indications that in diseased hearts, CV values can become considerably lower due to remodeling [12]. In this study, time-stepping was using Rush Larsen method for gating variables and explicit Euler for other dynamic variables and for diffusion as described previously [13]. The time step was taken to be 0.05 ms. This numerical scheme guarantees stability, provides sufficient accuracy, consistent with that of the underlying kinetic model, and ensures comparability with previous studies.

*Research supported by EPSRC (UK) (EP/I029664/1, EP/I029826/1, EP/I030158/1), and PRACE Introductory HPC Access (PRPB09, 2012). The calculations for this paper were performed using HECToR UK national supercomputing facility and the University of Exeter Supercomputer.

S Kharche and V N Biktashev are with CEMPS, University of Exeter, Exeter, EX4 4QF UK. (phone: 01392 726636; e-mail: S.R.Kharche@exeter.ac.uk).

I V Biktasheva is with Computer Science Department, University of Liverpool, Liverpool, L69 3BX, UK.

H Zhang is with Biological Physics, Physics Department, University of Manchester, Manchester, M13 9PL, UK.

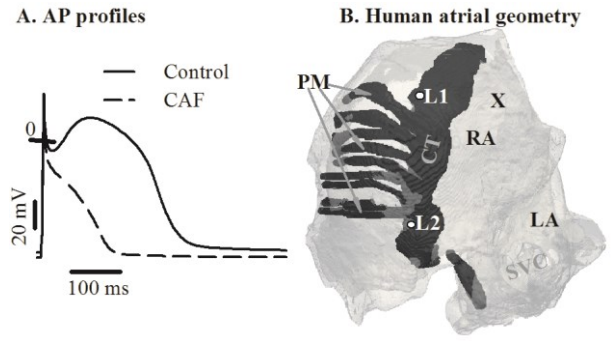

Fig 1. A: AP profiles under Control and CAF conditions. B: Anterior view of the human atrial geometry showing atrial tissue (translucent), and conduction pathways (black). The right atrium (RA), left atrium (LA), crista terminalis (CT), pectinate muscles (PM), and superior vena cava (SVC) are indicated. The initiation sites (shown as L1 and L2) and the registration electrode location (marked by "X") are also shown.

Scroll waves were initiated in the right atrium by means of the phase distribution method [14]. Two initiation sites (termed L1 and L2 shown in Fig. 1B) were used to highlight the effects of anisotropy. Location of registration electrode where the AP during scroll wave simulation was recorded is shown as "X" in Fig. 1B. The evolution of the scroll waves was quantified by means of scroll wave filament trajectory, recurrence maps of the consecutive cycle lengths (CL_n) of AP profile recordings [15], dominant frequency of AP recordings, and life span (LS) of scroll waves. The pacing duration was quantified as LS of scroll waves. The results obtained with anisotropy were compared to the results previously obtained in the isotropic case [5]. A total of 10 s of electrical activity was simulated in each simulation run. Re-entry in 2D isotropic sheets of atrial tissue under CAF conditions has been seen to be weakly meandering as opposed to rigidly rotating spirals [5]. In the 3D model, the meander and drifting pattern is complex. Therefore, in this study, the initial locations of the scroll wave filament (indicated by S in the 3D figures), the pinning locations (indicated by P), the meandering (indicated my M), and the final (indicated by F) are shown for clarity.

Scroll wave behaviour under Control and CAF conditions were characterized in multiple simulations. As the scroll waves under Control conditions self-terminated rapidly, cardioversion was not explored under Control conditions. The evolution of scroll waves under CAF conditions initiated at either L1 or L2 was computed. Then, the minimum amount of a single current shock required for instant elimination of the CAF scroll waves, defined as the stimulation threshold, was estimated. This was done by applying an external stimulus after allowing the CAF scroll waves to become established for 1.5 s of simulated activity.

The strength of the threshold stimulation was explored in the range of 3 pA/pF to 6 pA/pF in steps of 0.5 pA/pF. Pursuant the theory, a smaller stimulus than the threshold stimulus was used to evaluate the effectiveness of low energy defibrillation using the following pacing protocol [5]. Every

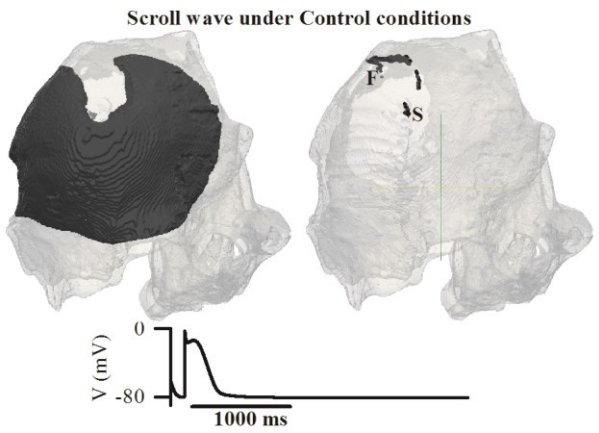

Fig. 2. Scroll waves under Control conditions. Top left panel shows a representative frame from the 3D simulation where translucent gray represents atrial geometry and black shows the scroll wave. Top right panel shows the filament trajectory (black symbols) with its starting location (S) and its end location (F) superimposed on atrial geometry (translucent gray). The AP recording during the simulation is shown in bottom panel.

instant when an excitation was registered or recorded by the registration electrode, a low amplitude (i.e. low energy) global stimulus was applied to the complete 3D model to induce migration of the scroll wave towards model boundaries, or cause elimination of scroll wave filament.

The tips of filaments were defined by conditions for the transmembrane voltage, V_m = -40 mV, and the transient outward current inhibition gating variable, o_i = 0.5, on the atrial surface nearest to the viewer, and calculated using the algorithm described in [16]. The 3D visualization was carried out using ParaView [17]. The AP profiles were analysed to obtain cycle length (CL) of consecutive excitations recorded at the registration electrode and recurrence maps (CL_{n+1} *vs* CL_n) was plotted [15].

III. Results

Scroll waves under Control conditions when initiated at location L1 are illustrated in Fig 2. The scroll wave self-terminated rapidly within 500 ms of initiation. This is marginally shorter than the LS of 650 ms in the isotropic case. The filament trajectory meandered over a small area before the scroll wave self-terminated and the filament was extinguished (Fig. 2). The behaviour of scroll waves initiated at L2 under Control conditions was similar.

A stimulation amplitude of 4.5 pA/pF was required to eliminate scroll wave activity both in the isotropic and anisotropic variants, indicating that in our model, the mono-domain threshold of the single-shock cardioversion, measured in terms of the transmembrane voltage, is not influenced by anisotropy. Note that this is separate from the effects of the anisotropy onto the conversion from external electric field to transmembrane voltage, which requires bidomain description, see e.g. [18].

Scroll waves under CAF conditions initiated at location L1 (Fig 3). The initiation sites are indicated by "S" in panels

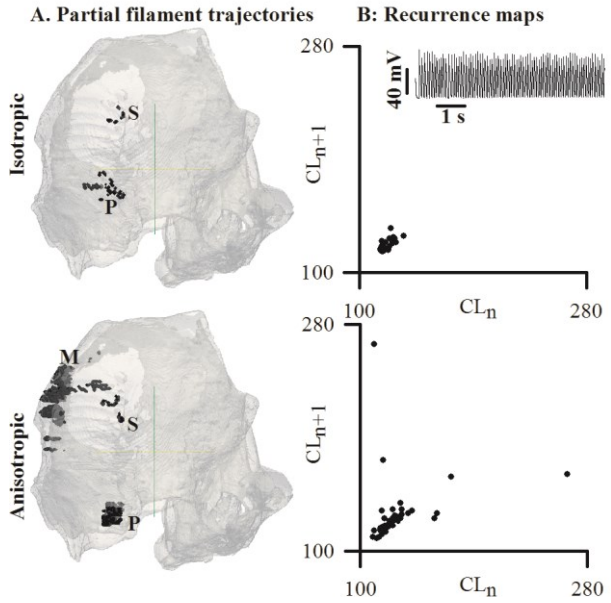

Fig. 3. CAF scroll waves with isotropic in the top row and anisotropic in the bottom row. A: Filament trajectories at the initial (S), meandering (M) and pinned (P) stages of the 10 s simulations. B: Recurrence maps of simulations shown in A. Representative AP recording is shown inset.

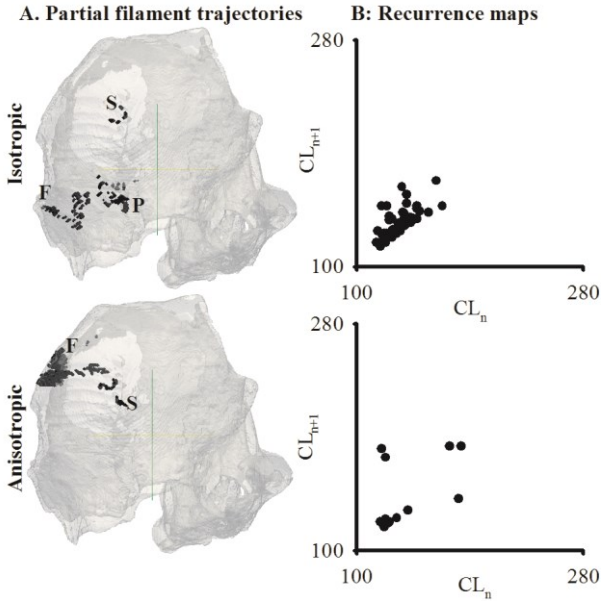

Fig. 4. Termination of CAF scroll waves with 1 pA/pF feedback stimulation. Isotropic data are shown in the top row and anisotropic data in the bottom row. A: Filament trajectories at the initial (S) and (F) stages of the 10 s simulations. B: Recurrence maps of simulations shown in A.

of Fig 3A. As in the isotropic case, the scroll wave in the anisotropic case was persistent for the 10 s duration of simulated electrical activity. However, the meander of the scroll wave in the isotropic and anisotropic cases was markedly different. In the isotropic case, the scroll wave steadily meandered for 3 s and then pinned to an anatomical site after 3 s (Fig. 3, top panel, indicated by "P"). The recurrence map of the AP recording shows that, in the isotropic case, the pinned scroll gives an almost monomorphic fibrillation. In the anisotropic case on the other hand, the mother rotor scroll initiated at L1 moved rapidly parallel to one of the pectinate muscles. After meandering in the region shown as M (Fig. 3, bottom panel) for a prolonged duration (5 s), the arm of the scroll wave gave rise to secondary scroll waves which became pinned to a blood vessel opening, as indicated by "P" in the bottom panel of Fig. 3A. The secondary scroll wave (not shown) was pinned to one of the blood vessel opening. The large meander and polymorphic nature of the tachycardia is reflected in the return maps. In both cases of isotropy and anisotropy, the maximum atrial pacing rates were found to be 8.5 Hz with secondary peaks in the power spectrum density close to the primary peak of 8.5 Hz, which matches clinical findings [19].

Low energy cardioversion was then simulated with scroll wave initiation at L1 (Fig. 4). A stimulus strength of 1 pA/pF was used, as it seen to be the minimum required in the isotropic case [5]. In the isotropic case, the scroll wave meandered towards the pinning site. It remained pinned for a prolonged duration (9 s into the simulated time of electrical activity). However, its meander progressively increased. Eventually, it became unpinned and rapidly migrated towards an anatomical boundary and was eliminated.

The exit location of the filament is marked by "F" in the top panel of Fig. 4A. The recurrence map shows a progressive increase of CL, indicating the effects of the feedback controlled stimulation. Successful cardioversion was seen with the stimulated scroll wave having a LS of 9.5 s. In the anisotropic case, the scroll wave that was initiated at L1 already had a propensity to migrate along the pectinate muscle fiber direction. Thus, application of far fewer stimuli was required to eliminate the scroll wave activity in the anisotropic case. Indeed, a much smaller amplitude stimulus of 0.2 pA/pF was found to be sufficient to eliminate the scroll wave within 3 s (LS) of simulated electrical activity. The recurrence map shows a large variation of CL. The maximum pacing rates were found to be marginally lower (7.5 to 8 Hz) in the stimulated cases than in the non-stimulated cases.

To confirm the effects of anisotropy on CAF scroll waves and cardioversion, scroll waves initiated at L2 (Fig. 1B) were studied. It was found that in the CAF scroll waves swiftly meandered to a pinning location (Fig 5, top panel). It remained in the pinned location for almost the complete duration of the 10 s of simulated electrical activity. Using stimulation strength of 1 pA/pF was found to be sub-optimal and insufficient to unpin the scroll wave, much less terminate it by means of a slow meander. The recurrence map (Fig 5B) shows that the pinning was strong and the CL of consecutive APs did not change significantly. Using stimulation strength of 2 pA/pF, the scroll wave still remained pinned for 2 s (Fig 5, bottom panels, pinning location shown by P) but was eventually unpinned and finally eliminated at a blood vessel boundary. The recurrence map reflects the large meander with consecutive APs being significantly different from each other. A power spectrum density of the AP recording showed

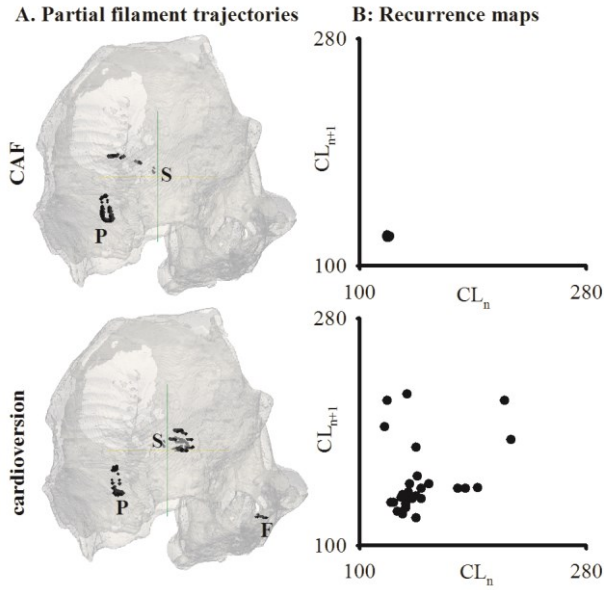

Fig. 5. CAF scroll waves initiated at L2. Top panels show CAF data while bottom panel shows cardioversion data when 2 pA/pF stimulation strength was used. A: Filament trajectories at the initial (S) and (F) stages of the 10 s simulations. B: Recurrence maps of simulations shown in column A.

that the scroll wave paced atrial tissue at pacing rates between 7 and 8 Hz.

IV. Conclusions and Limitations

The simulation results demonstrate the significant role of anisotropy in the human atria. Under Control conditions, it seems to facilitate hyper meander of scroll waves causing rapid self-termination. In the diseased state, anisotropy leads to polymorphic tachycardia and a persistent combination of mother rotors and secondary erratic propagations. The scroll waves location significantly affects the strength and pacing duration of the external stimulation necessary for scroll wave termination. Further investigation will assist in evaluating an optimal cardioversion protocol. The simulation results show that anatomy as well as anisotropy have a significant role in the persistence (or otherwise) of scroll waves in the atria. Although the role of stimulation strength and the location of scroll waves in cardioversion were explored, further cardioversion parameters will be quantified in future studies. One of the limitations related to model uncertainties is the choice of diffusivities, determining the CV. Naturally, any changes of model parameters may necessitate changes in the computational scheme. Another limitation is that the fiber direction in the anatomical model [10] of human atria was incorporated using rule based methods due to lack of resolution in the source photographic image data.

References

[1] J. N. Weiss, Z. Qu, P. S. Chen, S. F. Lin, H. S. Karagueuzian, H. Hayashi, A. Garfinkel, and A. Karma, "The dynamics of cardiac fibrillation," *Circulation,* vol. 112, pp. 1232-40, Aug 23 2005.

[2] V. N. Biktashev and A. V. Holden, "Design principles of a low voltage cardiac defibrillator based on the effect of feedback resonant drift," *J Theor Biol,* vol. 169, pp. 101-12, Jul 21 1994.

[3] I. V. Biktasheva, D. Barkley, V. N. Biktashev, G. V. Bordyugov, and A. J. Foulkes, "Computation of the response functions of spiral waves in active media," *Phys Rev E Stat Nonlin Soft Matter Phys,* vol. 79, p. 056702, May 2009.

[4] I. V. Biktasheva, D. Barkley, V. N. Biktashev, and A. J. Foulkes, "Computation of the drift velocity of spiral waves using response functions," *Phys Rev E Stat Nonlin Soft Matter Phys,* vol. 81, p. 066202, Jun 2010.

[5] S. Kharche, I. V. Biktasheva, H. Zhang, and V. N. Biktashev, "Cardioversion in the Human Atria: A Simulation Study," *Cinc: 2012 Annual Computers in Cardiology Conference,* 2012.

[6] O. V. Aslanidi, M. A. Colman, J. Stott, H. Dobrzynski, M. R. Boyett, A. V. Holden, and H. Zhang, "3D virtual human atria: A computational platform for studying clinical atrial fibrillation," *Prog Biophys Mol Biol,* vol. 107, pp. 156-68, Oct 2011.

[7] R. McFarlane and I. V. Biktasheva, "Beatbox—A Computer Simulation Environment for Computational Biology of the Heart," in *Visions of Computer Science— BCS International Academic Conference*, London, 2008, pp. 99-109.

[8] M. Courtemanche, R. J. Ramirez, and S. Nattel, "Ionic mechanisms underlying human atrial action potential properties: insights from a mathematical model," *Am. J. Physiol.,* vol. 275, pp. H301-21, Jul 1998.

[9] A. J. Workman, K. A. Kane, and A. C. Rankin, "The contribution of ionic currents to changes in refractoriness of human atrial myocytes associated with chronic atrial fibrillation," *Cardiovasc Res,* vol. 52, pp. 226-35, Nov 2001.

[10] G. Seemann, C. Hoper, F. B. Sachse, O. Dossel, A. V. Holden, and H. Zhang, "Heterogeneous three-dimensional anatomical and electrophysiological model of human atria," *Philos Transact A Math Phys Eng Sci,* vol. 364, pp. 1465-81, Jun 15 2006.

[11] F. M. Weber, A. Luik, C. Schilling, G. Seemann, M. W. Krueger, C. Lorenz, C. Schmitt, and O. Dossel, "Conduction velocity restitution of the human atrium--an efficient measurement protocol for clinical electrophysiological studies," *IEEE Trans Biomed Eng,* vol. 58, pp. 2648-55, Sep 2011.

[12] H. M. van der Velden and H. J. Jongsma, "Cardiac gap junctions and connexins: their role in atrial fibrillation and potential as therapeutic targets," *Cardiovasc Res,* vol. 54, pp. 270-9, May 2002.

[13] R. H. Clayton and A. V. Panfilov, "A guide to modelling cardiac electrical activity in anatomically detailed ventricles," *Prog Biophys Mol Biol,* vol. 96, pp. 19-43, Jan-Apr 2008.

[14] V. N. Biktashev and A. V. Holden, "Reentrant waves and their elimination in a model of mammalian ventricular tissue," *Chaos,* vol. 8, pp. 48-56, Mar 1998.

[15] F. Xie, Z. Qu, J. Yang, A. Baher, J. N. Weiss, and A. Garfinkel, "A simulation study of the effects of cardiac anatomy in ventricular fibrillation," *J Clin Invest,* vol. 113, pp. 686-93, Mar 2004.

[16] M. Dowle, R. M. Mantel, and D. Barkley, "Fast simulations of waves in three-dimensional excitable media," *International Journal of Bifurcation and Chaos,* vol. 7, pp. 2529-2545, Nov 1997.

[17] A. Henderson, *ParaView Guide, A Parallel Visualization Application.*: Kitware Inc., 2007.

[18] N. H. Kuijpers, R. H. Keldermann, T. Arts, and P. A. Hilbers, "Computer simulations of successful defibrillation in decoupled and non-uniform cardiac tissue," *Europace,* vol. 7 Suppl 2, pp. 166-77, Sep 2005.

[19] Y. J. Lin, H. M. Tsao, S. L. Chang, L. W. Lo, Y. F. Hu, C. J. Chang, W. C. Tsai, K. Suenari, S. Y. Huang, H. Y. Chang, T. J. Wu, and S. A. Chen, "Role of high dominant frequency sites in nonparoxysmal atrial fibrillation patients: insights from high-density frequency and fractionation mapping," *Heart Rhythm,* vol. 7, pp. 1255-62, Sep 2010.